Talanta 101 (2012) 45–52

Contents lists available at SciVerse ScienceDirect

Talanta

journal homepage: www.elsevier.com/locate/talanta

Adsorption of heavy metal ions by hierarchically structured magnetite-carbonaceous spheres

Jingming Gong [a,*], Xiaoqing Wang [a], Xiulan Shao [a], Shuang Yuan [a], Chenlin Yang [a], Xianluo Hu [b]

[a] Key Laboratory of Pesticide & Chemical Biology of Ministry of Education, College of Chemistry, Central China Normal University, Wuhan 430079, PR China
[b] State Key Laboratory of Material Processing and Die & Mould Technology, College of Materials Science and Engineering, Huazhong University of Science and Technology, Wuhan 430074, PR China

ARTICLE INFO

Article history:
Received 4 April 2012
Received in revised form
18 August 2012
Accepted 27 August 2012
Available online 3 September 2012

Keywords:
Heavy metal ions
Separation technology
Magnetite
Carbonaceous composites
Adsorption

ABSTRACT

Magnetically driven separation technology has received considerable attention in recent decade for its great potential application. In this work, hierarchically structured magnetite-carbonaceous microspheres (Fe_3O_4-C MSs) have been synthesized for the adsorption of heavy metal ions from aqueous solution. Each sphere contains numerous unique rattle-type structured magnetic particles, realizing the integration of rattle-type building unit into microspheres. The as-prepared composites with high BET surface area, hierarchical as well as mesoporous structures, exhibit an excellent adsorption capacity for heavy metal ions and a convenient separation procedure with the help of an external magnet. It was found that the maximum adsorption capacity of the composite toward Pb^{2+} was $\sim$126 mg g^{-1}, displaying a high efficiency for the removal of heavy metal ions. The Freundlich adsorption isotherm was applicable to describe the removal processes. Kinetics of the Pb^{2+} removal was found to follow pseudo-second-order rate equation. The as-prepared composite of Fe_3O_4-C MSs as well as Pb^{2+}-adsorbed composite were carefully examined by scanning electron microscopy (SEM), Zeta potential measurements, Fourier transform infrared spectroscopy (FT-IR), nitrogen sorption measurements, and X-ray photoelectron spectroscopy (XPS). Based on the characterization results, a possible mechanism of Pb^{2+} removal with the composite of Fe_3O_4-C MSs was proposed.

1. Introduction

It is well known that heavy metal ions such as Pb^{2+}, Cd^{2+}, Cr^{3+}, Ni^{2+} and Hg^{2+} pose a great threat to ecological and human health since they may easily bind proteins, nucleic acid, and small metabolites in living organisms [1]. Owing to their long-term environmental toxicity and short-term public health damage, the removal of such toxic metal ions from natural water has generated considerable concern by researchers worldwide [2–5]. Various treatment technologies have been used for water contaminated by heavy metals, including chemical precipitation, solvent extraction, reverse osmosis, ion-exchange, filtration, electrodialysis, and so on [6–9]. Each method, however, has been found to be limited by cost, complexity, and efficiency as well as secondary waste. Sorption technology is regarded as one of the most promising technologies owning to its cost-effective, versatile and simple to operate for removing trace levels of heavy metal ions. Great efforts have been made to develop new adsorbents such as activated carbons [10–12], granular titanium dioxide [13], activated alumina [14], zeolites [15], calix arenes [16], layered double hydroxides-based nanoassembly [17], and various biomasses [18,19], etc. As known, one of the ultimate goals for the pollutant removal is to design and fabricate highly efficient adsorbents with high adsorption capacity, and rapid adsorption rate.

In recent years, the discovery of the hierarchically structured materials has initiated intensive interest for wastewater treatment [20–22]. Their novel structures possess a high surface to bulk ratio and a large surface area, contributing to high adsorption capacities and fast adsorption rates as well as remarkably facilitating the mass transportation of the targets. Several groups have successfully applied the synthesized hierarchically structured materials for removing contamination. For example, Li et al. synthesized hierarchical hollow nanostructures of manganese oxide for water decontamination [21]. Hierarchical meso-/macroporous aluminum phosphonate composites were reported to be a viable multifunctional adsorbent [22]. The applications of such hierarchically structured materials, however, are always restricted by the difficult solid–liquid separation. To facilitate the separation process during the decontamination, magnetic separation has become one of the promising ways [23–27]. Recently, the hierarchically structured magnetic materials, integrating the hierarchically structure with magnetic properties,

* Corresponding author. Tel./fax: +86 27 6786 7535.
E-mail address: jmgong@mail.ccnu.edu.cn (J. Gong).

0039-9140/$ - see front matter © 2012 Elsevier B.V. All rights reserved.
http://dx.doi.org/10.1016/j.talanta.2012.08.035

have shown remarkable potential to treat large amount of wastewater within a short time and can be conveniently separated from wastewater [28–30].

Herein, we synthesized hierarchically magnetic carbonaceous microspheres (Fe_3O_4-C MSs) by a facile injection-assisted approach coupled with a simple annealing procedure and systematically studied the adsorption performance toward heavy metal ions. The non-toxic and biodegradable chitosan is chosen as a carbon precursor. By calcination at an elevated temperature, the as-synthesized precursor of iron oxide-chitosan (Fe_2O_3-chi) was further transformed into magnetite-carbonaceous microspheres. Interestingly, each sphere contains numerous uniform rattle-type structured particles. As a unique building unit of the hierarchical structure, rattle-type materials, with a remarkable cavity volume between the yolk and the shell, could provide additional room for loading targets owing to interstitial space between shells and cores [29,31,32], significantly improving the loading capacity toward the targets. It is expected that rattle-type magnetic materials, combining the merits of the high loading capacity (from hierarchical structures) and the targeted delivery properties (from magnetic particles), could dramatically facilitate the enrichment of targets and realize the highly-efficient decontaminations. To the best of our knowledge, this is the first report on the synthesis of the hierarchically rattle-type magnetic carbonaceous microspheres and further exploring their fine applicability for the removal of heavy metal ions (such as Pb^{2+}, Cd^{2+}, and Cr^{3+}) from simulated water samples. After adsorption of analytes, they can be quickly isolated from solution under an external magnetic field, avoiding the tedious procedures associated with the powder (such as centrifugation or isolation, or adhesion onto the supporter, etc) as the adsorbents. The factors such as pH, initial concentration, adsorption isotherms and kinetics, as well as desorption/reuse were investigated in detail and the applicability of these sorbents was evaluated by the analysis of trace metal Pb^{2+} in environmental water samples.

2. Experimental section

2.1. Materials

Chitosan from crab shells (85% deacetylated) was purchased from Sigma. $Fe(NO_3)_3 \cdot 9H_2O$, sodium hydroxide, CH_3COOH, and $Pb(NO_3)_2$, were obtained from National Medicines Corporation Ltd. of China. All the chemicals were of analytical grade and were used as received without further purification. Deionized water was used throughout the experiments.

2.2. Instruments

X-ray diffraction (XRD) patterns were collected with a Rigaku Ultima III X-ray diffractometer with high-intensity Cu $K_{\alpha 1}$ irradiation ($\lambda = 1.5406$ nm). The general morphology of the product was characterized by the scanning electron microscopy (SEM, JSM-5600). The magnetic properties of the as-prepared magnetite-carbonaceous microspheres were investigated using a Lake model 7300 vibrating sample magnetometer (VSM). X-ray photoemission spectroscopy was recorded on a Kratos standard and monochromatic source (Al Kα) operated at 150 W (15 KV, 10 mA). FT-IR spectra were recorded on a Nicolet Nexus spectrometer with the standard KBr pellet method. Nitrogen adsorption–desorption isotherms were collected on a Micromeritics Tristar-3000 surface area and porosity analyzer at 77 K after the sample had been degassed in the flow of N_2 at 180 °C for 5 h. The BET surface area was calculated from the linear part of the BET plot. pH values were measured with an Orion model PHS-25 m.

2.3. Preparation of Fe_2O_3-chi and Fe_3O_4-C MSs

The precursor of Fe_2O_3-chi spheres were synthesized by a channel injection-assisted approach, according to the previous literatures reported on the synthesis of the gelled chitosan composite spheres [33–35]. Briefly, 1.5 g of chitosan was first dissolved in 50 mL of 3% (v/v) acetic acid, followed by adding 3.6 mL of $FeCl_3$ (0.5 M) solution. The homogeneous solution was obtained under vigorous magnetic stirring. Then the resulting solution was added dropwise into a NaOH solution (3 M) through a needle ($\varphi = 0.5$ mm) equipped with a syringe pump. An optimal drop height of about 6 cm was set to obtain spherical products, and the gelled spheres were formed instantaneously. The formed spheres were washed with deionized water thoroughly and then dried at 50 °C overnight, leading to the precursor of Fe_2O_3-chitosan composites (Fe_2O_3-chi) obtained. Finally, the products were annealed at 600 °C in nitrogen atmosphere. The whole synthesis procedure for magnetite-carbonaceous microspheres (Fe_3O_4-C MSs) is presented in Scheme 1.

2.4. Experiments for removal of heavy metal ions

The stock aqueous solutions containing 1000 mg L^{-1} of different heavy metal ions (Pb^{2+}, Cd^{2+}, and Cr^{3+}) were prepared. Typically, simulated wastewater with different Pb^{2+} concentrations (2.0, 4.0, 6.0, 8.0, 10.0 mg L^{-1}) was prepared by dilution of the stock $Pb(NO_3)_2$ standard solution. Then, 100 mg of Fe_3O_4-C MSs was added to 100 mL of the solutions with different Pb^{2+} concentrations. After the adsorption processes, the samples were separated using the magnetic field, and the filtrates were immediately analyzed by atomic absorption spectrometry (WFX-1F2, China). The adsorption of Cd^{2+}, and Cr^{3+} was determined similarly. All the adsorption experiments were carried out in duplicate. The relative deviations are in the range of $\pm 5.0\%$. The initial pH of Cu^{2+} solution was 6.08 without pH adjustment. In some cases, the initial pH values of the Pb^{2+} solution were adjusted from 2 to 8 by addition of 0.1 M HCl and 1 M NaOH. The amount of Pb^{2+} ions adsorbed per unit mass of the adsorbent was evaluated by using the mass balance equation

$$qt = (C_0 - C_t)V/W \quad (1)$$

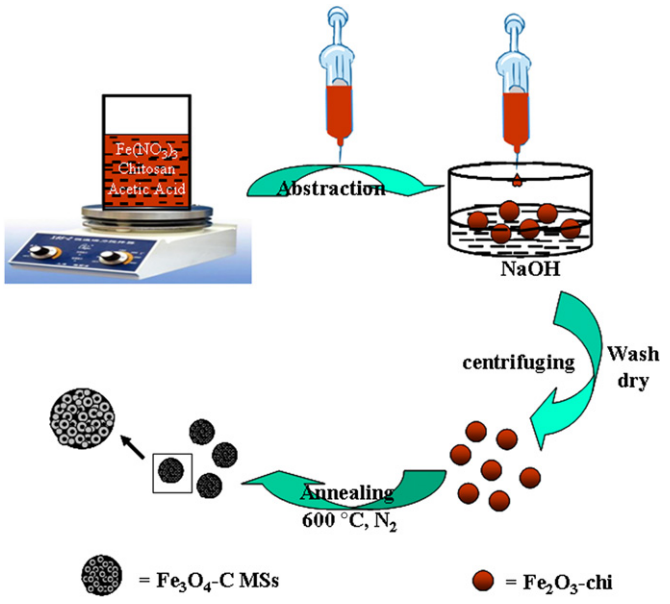

Scheme 1. Schematic illustration for the preparation of Fe_3O_4-C MSs in an injection-assisted approach coupled with a simple annealing process.

where q_t (mg g^{-1}) is the amount adsorbed per gram of adsorbent at time t ($_{min}$), C_0 is the initial concentration of Pb^{2+} in the solution (mg L^{-1}), C_t is the concentration of Pb^{2+} at time t of adsorption (mg L^{-1}), W is the mass of the adsorbent used (g), and V (L) is the initial volume of the Pb^{2+} solution.

3. Results and discussion

3.1. Characterization of the as-prepared product

The precursor of Fe_2O_3-chitosan composites (Fe_2O_3-chi) was firstly synthesized. After a simple annealing procedure, the crystallinity of the resulting magnetite-carbonaceous microspheres (Fe_3O_4-C MSs) was characterized by XRD analysis. As shown in Fig. 1, a weak broad peak centered at ~22.5° was observed, attributed to the amorphous phase of carbon [36]. The characteristic reflections at 2θ=30.10°, 35.30°, 37.09°, 42.90°, 53.46°, 56.76°, and 62.35°, correspond to the spinel structure of magnetite (Fe_3O_4, JCPDS no.75-1610). Obviously, through annealing, we have successfully synthesized the composite of magnetite-carbonaceous microspheres (Fe_3O_4-C MSs). The typical SEM images for Fe_3O_4-C MSs were shown in Fig. 2(A–C). It can be seen that Fe_3O_4-C MSs show a microsphere shape, ~0.4 μm in diameter. Interestingly, each sphere is made up of numerous uniform nanoparticles (~40 nm in size), indicating the hierarchical structure of the spheres with a rough surface. TEM studies (Fig. 2D) further disclose that each nanoparticle exhibits a typical rattle-type structure, leaving a ring cavity with a magnetic core of ~22 nm in diameter, and a carbon shell of ~12 nm in thickness.

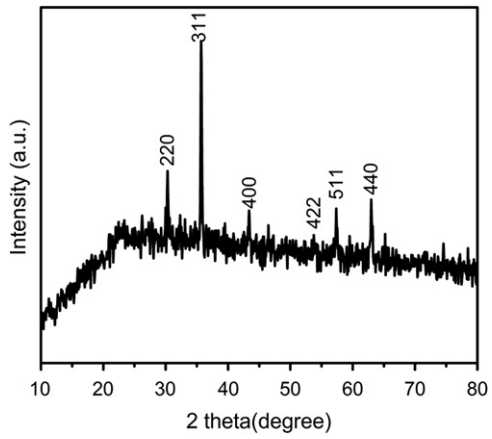

Fig. 1. XRD pattern of the as-prepared composite of Fe_3O_4-C MSs.

Magnetic properties of the Fe_3O_4-C MSs composites were studied using a vibrating sample magnetometer at room temperature in the applied magnetic field sweeping from −5 to 5 kOe (shown in Fig. 3). No hysteresis, remanence and neither coercivity was observed, implying the superparamagnetic nature. The superparamagnetic property of Fe_3O_4-C MSs efficiently ensures its application. For example, it could prevent the microspheres from aggregation and enable MSs to redisperse rapidly once the magnetic field is removed. The mild magnetic saturation value (~3.0 emu/g) may be contributed to the presence of carbon in the composite of Fe_3O_4-C MSs. Inset of Fig. 3 shows photographs of microspheres before (a) and after (b) magnetic separation using an external magnetic field. Such an excellent magnetic property provides an efficient way to separate Fe_3O_4-C MSs easily from the solution with the help of an external magnetic force.

The porous structure of the as-prepared Fe_3O_4-C MSs was studied by N_2 adsorption–desorption (shown in Supplementary data, Fig. S1). Fig. S1 displays typical IV adsorption isotherms with the hysteresis loop H1, indicative of a porous structure. The BET surface area of the as-prepared Fe_3O_4-C MSs was found to reach 206.6 m^2/g. Such a high surface area may be attributed to the unique hierarchical structure of Fe_3O_4-C MSs. The BJH analysis shows the presence of mesopores with an average pore diameter of ~40 nm, filling the sample of Fe_3O_4-C MSs. Both the high BET surface area and the hierarchical and mesoporous structure would undoubtedly facilitate the ion adsorption, exchange, and

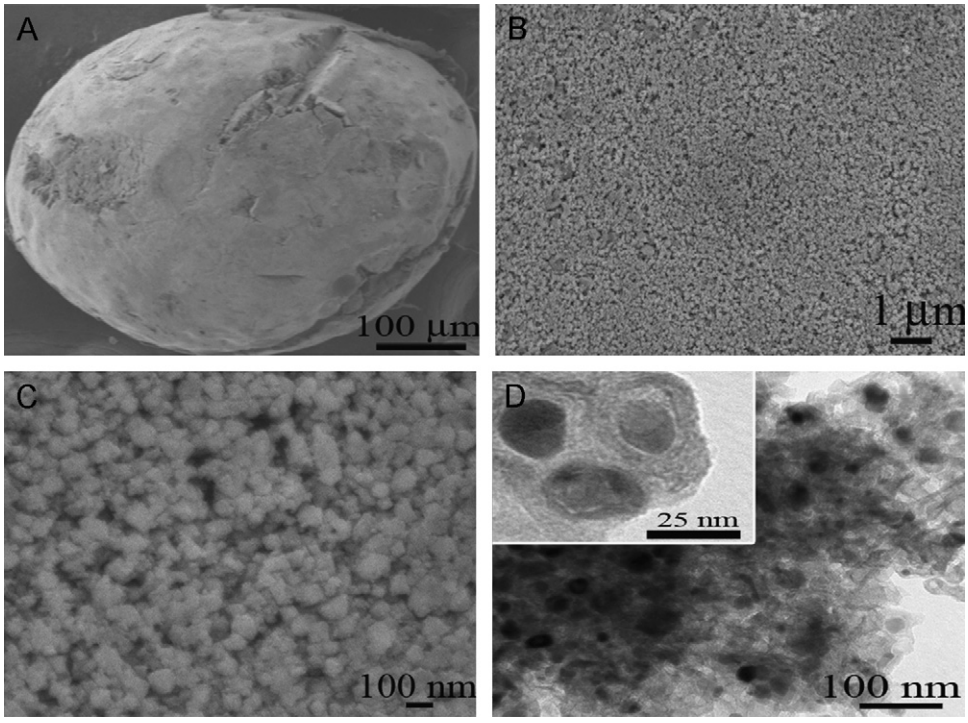

Fig. 2. (A) Low-magnification, (B) and (C) enlarged SEM images of a single sphere of Fe_3O_4-C spheres, and (D) TEM image of the dispersed as-prepared Fe_3O_4-C MSs.

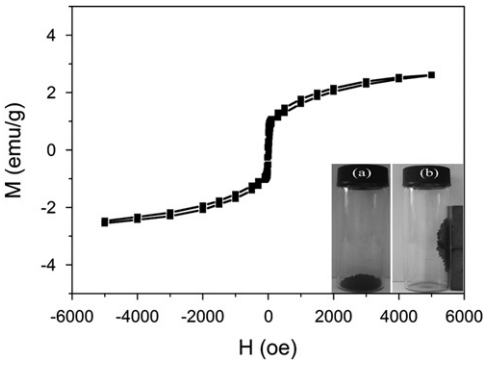

Fig. 3. Hysteresis loops of the as-prepared sample of Fe_3O_4-C MSs; inset: photographs of the as-prepared magnetic sample of Fe_3O_4-C MSs attracted by an external magnet.

diffusion. It is expected that the resulting Fe_3O_4-C MSs could afford the high-performance decontamination capability.

3.2. Removal of heavy metal ions

To investigate the removal capacity of the as-prepared Fe_3O_4-C MSs samples, toxic metal ions such as Cr^{3+}, Cd^{2+}, and Pb^{2+} ions in water solution were used. It can be found that the removal of Cr^{3+} is the quickest, almost finished within ~5 min, the rate followed in the order of $Cr^{3+} > Pb^{2+} > Cd^{2+}$. The whole removal process of Cr^{3+}, Cd^{2+}, and Pb^{2+} ions was almost finished within ~10 min using 1.0 g L^{-1} of Fe_3O_4-C MSs as scavengers, with high efficiency above ~97.0% at the initial metal ions concentrations of 10.0 mg L^{-1} (shown in Fig. 4A). The high removal efficiency is most likely related to the unique hierarchically rattle-type structure. A series of systematic experiments have been performed to examine the removal of Pb^{2+}. Fig. 4B) shows the time profile of Pb^{2+} removal with 1.0 g L^{-1} of Fe_3O_4-C MSs at different initial Pb^{2+} concentrations. It can be seen that the adsorption rates were considerably fast under all the concentrations. The adsorption process was almost finished within 13 min, and no significant change was observed from 13 to 120 min. The removal efficiencies were found to be 91.5%, 93.0%, 94.5%, 95.9% and 97.6% at the initial Pb^{2+} concentrations of 2.0, 4.0, 6.0, 8.0 and 10.0 mg L^{-1}, respectively. The maximum adsorption capacity of the assembly (Fe_3O_4-C MSs) toward Pb^{2+} was found to be 126 mg g^{-1}, which was significantly higher than 119 mg g^{-1} observed for activated carbons prepared from cotton stalk by Li and coworkers [37], and also higher than those obtained using Fe_3O_4 nanoadsorbents and calcined phosphate as an adsorbent (below 50 mg g^{-1}) [38,39]. The high efficiency of the Fe_3O_4-C MSs for the removal of Pb^{2+} ions in aqueous solutions may be attributed to the unique hierarchically rattle-type structure. On the other hand, seen from the removal time profile, with the increase of the initial Pb^{2+} concentrations, the total amount of Pb^{2+} adsorbed increased successively. It could be attributed that more targets of Pb^{2+} could provide a higher driving force to facilitate the ion diffusion from the solution to Fe_3O_4-C MSs, and more collisions between Pb^{2+} ions and active sites of the Fe_3O_4-C MSs. Similar phenomena have also been observed in the literature [17].

The influence of the initial solution pH on the removal of the Pb^{2+} ions by the Fe_3O_4-C MSs was investigated, illustrated in Fig. S2 (Supplementary data). It was found that the adsorption capacity increased upon increasing the pH value to pH 6.0 and then decreased. When the initial pH varied from 2 to 4, the removal efficiency of Pb^{2+} increased from 24.2 to 95.2%, but when the initial pH increased from 4.0 to 6.0, the adsorption efficiency of Pb^{2+} increased to 97.6%. If the pH value was

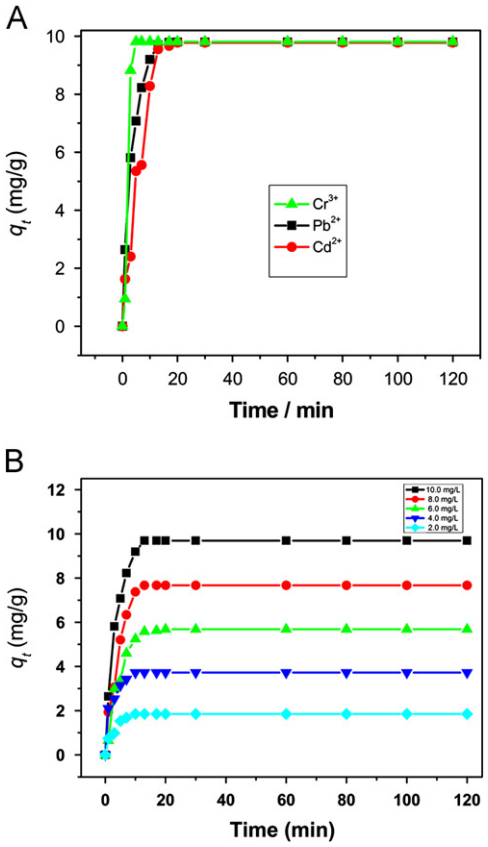

Fig. 4. (A) Time profile of Pb^{2+}, Cd^{2+} and Cr^{3+} removal with the composite of Fe_3O_4-C MSs microspheres. The initial metal ion concentration was 10.0 mg L^{-1}. (B) Time profile of Pb^{2+} removal with the composite of Fe_3O_4-C MSs. The initial Pb^{2+} concentrations ranged from 2.0 to 10.0 mg L^{-1}; the concentration of Fe_3O_4-C MSs adsorbent was 1.0 g L^{-1}.

enhanced from 6.0 to 8.0, the adsorption ability decreased greatly. This phenomenon may be explained as follow. Firstly, the structure of magnetite-carbon composites will be destroyed in a strong acidic solution, leading to the decreased adsorption affects toward Pb^{2+}. Secondly, heavy metal ions may form as many polynuclear species in water. For example, when pH > 6, hydrolysis of Pb^{2+} will occur and it will exist as $Pb_2(OH)^{3+}$ and $Pb_3(OH)^{4+}$. Both of hydrolysis and polymerizing of metal ions will reduce the adsorption capacity.

3.3. Adsorption isotherms

Both Langmuir and Freundlich isotherms were tried to describe the adsorption behavior of Pb^{2+} by Fe_3O_4-C MSs [40,41]. The Langmuir isotherm is often applicable to a homogeneous adsorption surface with all the adsorption sites having equal adsorbate affinity, while the Freundlich isotherm model assumes heterogeneity of adsorption surfaces, expressed by the Freundlich equation (Eq. (2)), where q_e and C_e are the amount of Pb^{2+} adsorbed (mg g^{-1}) and Pb^{2+} concentration at equilibrium, respectively. K and n are the Freundlich isotherm constants. K value indicates the adsorption capacity. n is related to the energetic heterogeneity (average energy of sites).

$$q_e = KC_e^{1/n} \quad (2)$$

Fig. 5A reveals that the adsorption data of Pb^{2+} on Fe_3O_4-C MSs fits well to Freundlich isotherm model with a correlation coefficient R^2 value of 0.998 and n value of 1.33 (between 1 and 10), representing beneficial adsorption [42]. For comparison, the

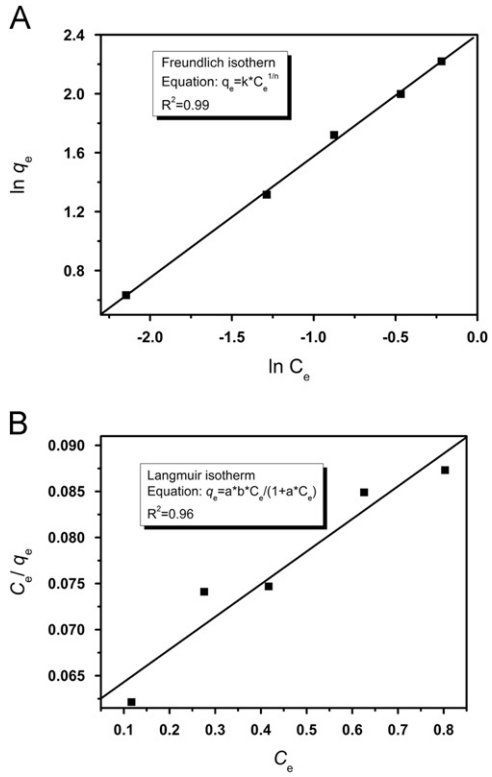

Fig. 5. Representative (A) Freundlich isotherm, and (B) Langmuir isotherm of Pb^{2+} adsorption. The initial Pb^{2+} concentrations were from 2.0 to 10.0 mg L^{-1}; the concentration of Fe_3O_4-C MSs adsorbent was 1.0 g L^{-1}.

Langmuir model was also used to fit the adsorption data. However, the resulting correlation coefficient of 0.96 was not as high as that of Freundlich model (Fig. 5B). The better fitting of the Freundlich isotherm model may be attributed to the heterogeneous distribution of active sites on the Fe_3O_4-C MSs surface [43].

3.4. Kinetics study

The kinetics of Pb^{2+} removal on the Fe_3O_4-C MSs was further investigated at various initial Pb^{2+} concentrations in the presence of 1.0 g L^{-1} of Fe_3O_4-C MSs. The pseudo-second-order rate constants (k_2) and the amount of Pb^{2+} adsorbed at equilibrium (q_e) were calculated from the slope and intercept of the plots of t/q_t versus t according to Eq. (3).

$$\frac{t}{q_t} = \frac{1}{k_2 q_e^2} + \frac{1}{q_e} t \quad (3)$$

where k_2 (g mg^{-1} min^{-1}) is the pseudo-second-order rate constant, q_e is the amount of Pb^{2+} adsorbed (mg g^{-1}) at equilibrium and q_t is the amount of the adsorption (mg g^{-1}) at any time t. The kinetics of the removal process was shown in Fig. 6. Table 1 summarizes the theoretical and calculated q_e values, pseudo-second order rate constants k_2, and correlation coefficient values (R^2). The calculated q_e is calculated from the slope and intercept of the plots of t/q_t versus t according to the Eq. (3). The theoretical q_e values are the equilibrium concentrations of Pb^{2+} in the adsorbed Fe_3O_4-C MSs, assuming 100% of Pb^{2+} is removed. The calculated q_e values were very close to the theoretical ones, showing quite good linearity with R^2 above 0.999. Therefore, the adsorption kinetics follows the pseudo-second-order model [44], suggesting a chemisorption process [45].

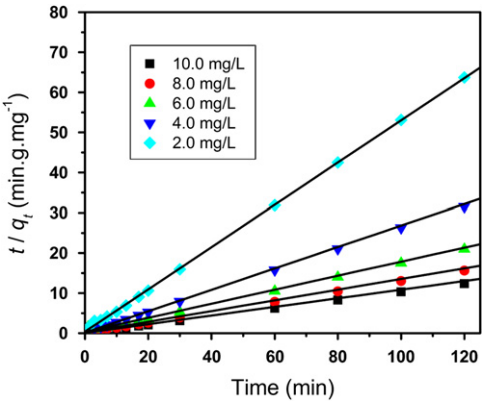

Fig. 6. Removal kinetics of 2.0, 4.0, 6.0, 8.0 and 10.0 mg L^{-1} of Pb^{2+} in the presence of 1.0 g L^{-1} Fe_3O_4-C MSs composite. The contact time was 2 h.

Table 1
Theoretical and calculated q_e Values, pseudo-second-order rate constants, k_2, and correlation coefficient values (R^2). The dosage of the composite of Fe_3O_4-C MSs adsorbent was 1.0 g L^{-1}.

Theoretical q_e (mg g^{-1})	Calculated q_e (mg g^{-1})	k_2 (g mg^{-1} min^{-1})	R^2	Standard deviation
2.0	1.871	0.6587	0.9998	0.4170
4.0	3.746	0.5270	0.9999	0.1209
6.0	5.711	0.09171	0.9991	0.3641
8.0	7.803	0.09053	0.9994	0.1740
10.0	9.830	0.08915	0.9998	0.08734

3.5. Possible adsorption mechanism of Pb^{2+} with Fe_3O_4-C MSs

Seen from the above results, the quick and efficient decontamination capability can be achieved using Fe_3O_4-C MSs. Obviously, the unique hierarchically rattle-type structure should play a crucial role. As to the uptake mechanism of metal ions by the Fe_3O_4-C MSs is still unknown. Further studies should be carried out to exploit the mechanisms for the Fe_3O_4-C MSs in remediation applications.

To confirm the surface charge, we measured the pH-dependent Zeta potential of the as-prepared Fe_3O_4-C MSs composite (Supplementary data, Fig. S3). It can be seen that electrostatic attraction between the negatively charged surface of Fe_3O_4-C MSs and the positively charged Pb^{2+} (at pH~6.0) plays a positive role, providing a viable approach to decontaminate Pb^{2+} by Fe_3O_4-C MSs.

X-ray photoelectron spectroscopy was further used to study the surface chemical compositions of the as-prepared and Pb^{2+}-adsorbed Fe_3O_4-C MSs (Fig. 7). Fig. 7A shows the two survey spectra before and after adsorption of Pb^{2+}. After adsorption, on one hand, the presence of Pb^{2+} on the surface of Fe_3O_4-C MSs was obviously observed; On the other hand, the binding energy (EB) values of C1s, N1s, O1s and Fe2p of the composite were remarkably shifted (a positive shift), respectively, indicating an alteration of the local bonding environments occurred. Likely, it is due to the specific adsorption of Pb^{2+} onto the surface of Fe_3O_4-C MSs. The high resolution XPS spectrum of the Fe2p peaks are shown in Fig. 7B, located at 711.29 and 724.28 eV, attributed to the characteristics Fe2p in Fe_3O_4 [46]. It is indicative of formation of the Fe_3O_4 phase in Fe_3O_4-C MSs composites, agreeing well with the XRD results. Fig. 7C shows the high resolution O1s spectrum before and after adsorption. One can see that before adsorption, the broad of peak of O1s can be fitted by two peaks at binding energies of 529.9 and 531.9 eV, respectively. The dominant peak at 529.9 eV is characteristics of oxygen in metal oxide of Fe_3O_4.

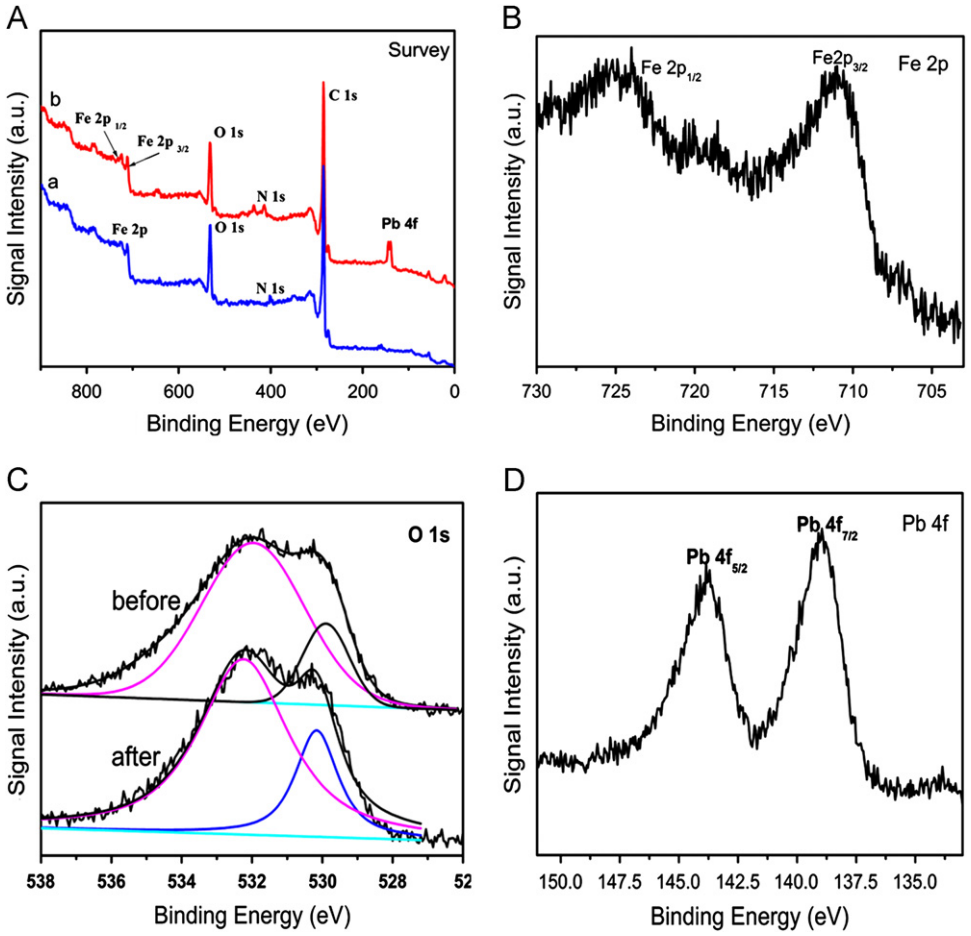

Fig. 7. XPS spectra of the composite of Fe_3O_4-C MSs of (A) survey: before (a) and after (b) Pb^{2+} adsorption; (B) high resolution XPS spectrum of Fe2p from Fe_3O_4-C MSs; (C) high resolution XPS of O1s: (a) before and (b) after the Pb^{2+} adsorption and (D) high resolution XPS spectrum of Pb4f for Pb^{2+}-adsorbed sample.

The other peak around at 531.9 eV suggests the presence of oxygen containing functional groups, such as –OH oxygen on the surface of Fe_3O_4-C MSs [27]. As known, generally, the heavy metal ions may be removed via i) surface adsorption (including electrostatic interactions, as well as complexation), and ii) the precipitation of metal hydroxides onto the surface of decontaminants. While the presence of oxygen containing functional groups (Sur-OH or Sur-O^-) exactly provides the feasibility to remove heavy metal ions by surface adsorption (Sur-OH-M^{n+} or Sur-O-M^{n+}, through the bonding with surface hydroxyl groups of adsorbent) or precipitation on the surface of decontaminants. Compared with O1s spectrum of Fe_3O_4-C MSs, after adsorption, the EB value of O1s of Pb^{2+}-adsorbed Fe_3O_4-C MSs indeed exhibits a positive shift, further confirming an alteration of the local bonding environments. Furthermore, the high resolution XPS spectrum of Pb4f peaks is observed to be located at 138.9, and 143.6 eV (Fig. 7D), revealing that the removal of Pb^{2+} was accompanied by the formation of lead hydroxide or lead carbonate hydroxide [47], that is, the precipitation of lead induced by the decontamination of Fe_3O_4-C MSs.

Fig. 8 shows the FTIR spectra of the as-prepared and Pb^{2+}-adsorbed Fe_3O_4-C MSs. The spectra display broad bands at $\sim$3440 cm^{-1}, which are believed to be associated with the stretching vibrations of surface hydroxyl groups of Fe_3O_4-C MSs (O–H stretching vibrations). One can see that a weak band was observed at 3440 cm^{-1} after adsorption. It is likely related with surface precipitation induced (lead hydroxide or lead carbonate hydroxide), leading to the decreased O–H stretching vibrations. The bands at 1635 cm^{-1} and 1562 cm^{-1} could be assigned to

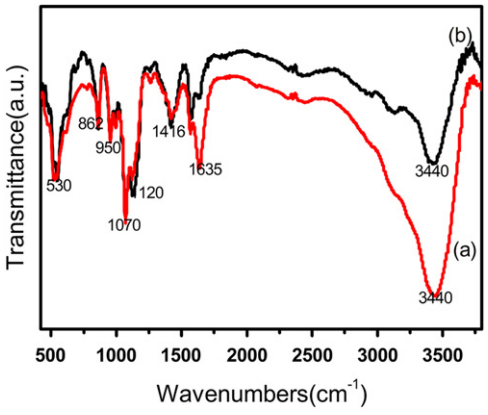

Fig. 8. Infrared spectra of (a) the as-prepared and (b) Pb^{2+}-adsorbed Fe_3O_4-C MSs.

N–H deformation vibrations (coming from the precursor of chitosan). Interestingly, we found that after adsorption, a band at 1635 cm^{-1} became obviously weakened. As known, the metal ions with empty orbital could be capable of accepting electron pairs, while the NH_2 groups having non-shared electron pairs, could donate their electron pair. It is ever reported that metal ions could be removed well through the chelation by the amide groups [35,48]. With the formation of Sur-NH_2-Pb^{2+} (chelating with surface amide), it is reasonable for the weakened bonding of N–H. The peak at 1416 cm^{-1} is attributed to C–H bending model of the alkyl chain. The bands observed at 500–900 cm^{-1} are due to

M–O lattice vibrations from Fe_3O_4-C MSs composite. For the bands in the range of 1000–1300 cm^{-1}, they are mainly due to the C–OH stretching vibrations, implying the existence of a certain amount of residual hydroxyl groups in the composite. It further confirmed the possibilities to form the complex of Sur-OH-Pb^{2+} or Sur-O-Pb^{2+} during the adsorption process. Moreover, an intensified band was observed at 1120 cm^{-1} after adsorption. It seems that the adsorption induces the increase of the amount of surface hydroxyl groups, which may arise from the formation of the surface precipitate of $Pb(OH)_2$ on the composite. Obviously, the above results not only disclose that through a simple annealing procedure toward the precursor (Fe_2O_3-chi), the obtained hierarchical and mesoporous composite (Fe_3O_4-C MSs) occupies abundant dehydrated residues, such as –OH and $–NH_2$ groups on the surface, greatly facilitating the adsorption of metal ions to the surface.

It has also been demonstrated that the removal of heavy metal ions by Fe_3O_4-C MSs was not a single process, mainly controlled by surface adsorption, including electrostatic interactions, surface complexation (such as bonding with surface hydroxyl and amide groups), as well as surface precipitation. The different adsorption rate of the composite toward Cr^{3+}, Pb^{2+} and Cd^{2+} also confirms this point. Whether from the point of the electrostatic interactions or surface precipitation ($K_{spCr(OH)_3} = 6 \times 10^{-30} > K_{spPb(OH)_2} = 1.2 \times 10^{-15} > K_{spCd(OH)_2} = 2.5 \times 10^{-14}$), it is reasonable for the adsorption performance in the order of $Cr^{3+} > Pb^{2+} > Cd^{2+}$. Such a porous Fe_3O_4-C composite exhibits remarkably high adsorption capacity and efficiency on the removal of heavy metal ions, providing a high-performance source and promising candidate for water decontamination.

3.6. Recycle and the analysis of the real samples performance of the composite of Fe_3O_4-C MSs

Desorption studies of Pb^{2+} from the composite were carried out to evaluate the regeneration behavior of the adsorbent. The samples of Pb^{2+}-adsorbed Fe_3O_4-C MSs were immersed into 25 mL weak acetum solution and sonicated the mixture for 1 h at room temperature. Pb^{2+} released into the solution was analyzed by using atom absorption spectrometry. It was found that about 96.3% of the adsorbed Pb^{2+} could be released to the eluent. Then, the separated samples were treated with deionized water and were further explored for Pb^{2+} removal in the succeeding cycles. We repeated above procedures up to five cycles. Although the removal efficiency is reduced gradually in the later cycles (Supplementary data, Fig. S4), it still could be found that the removal efficiency of 91% still remained in the final cycle, indicating a good recycle performance of the used composite of Fe_3O_4-C MSs.

To further demonstrate the practicality of the present sorbent, it was evaluated by processing tap and lake water samples. Lake water was sampled from the central part of East Lake (Wuhan, China) and treated through a standard 0.45 μm filter. The analytical results, along with the recovery for the spiked samples, are summarized in Table S1 (Supplementary data). As can be seen, recoveries for the target analytes ranged from 96.5% to 103% for the real samples, indicating the feasibility of Fe_3O_4-C MSs composite for direct analysis of relevant real samples.

4. Conclusions

In summary, the present work explored a novel hierarchically structured magnetite-carbonaceous adsorbent (Fe_3O_4-C MSs) toward the removal of heavy metal ions. The composite of Fe_3O_4-C MSs has been successfully fabricated via a channel injection-assisted approach coupled with a simple annealing procedure. The resulting composites, featuring a high BET surface area, hierarchical as well as mesoporous structures, and convenient separation from water with the help of an external magnet, display fine applicability for removing heavy metal ions from simulated water samples. We also proposed the possible mechanism of removal of Pb^{2+} with the hierarchical composite of Fe_3O_4-C MSs, mainly controlled by surface adsorption and precipitation. This study presents a good example of exploring hierarchical Fe_3O_4-C MSs as a versatile and promising candidate for the removal of heavy metal ions from simulated water samples.

Acknowledgements

This work was supported by the National Science Foundation of China (Grant 20803026, 21175053), the Program for Chenguang Young Scientist for Wuhan (201271031412) and Self-determined Research Funds of CCNU from the Colleges' Basic Research and Operation of MOE (Grant CCNU10A01006).

Appendix A. Supporting information

Supplementary data associated with this article can be found in the online version at doi:10.1016/j.talanta.2012.08.035.

References

[1] R.P. Schwarzenbach, B.I. Escher, K. Fenner, T.B. Hofstetter, C.A. Johnson, U. Gunten, B. Wehrli, Science 313 (2006) 1072.
[2] W.C. Chang, G.S. Hsu, S.M. Chiang, M.C. Su, Bioresour. Technol. 97 (2006) 1503.
[3] C.C. Huang, H.T. Chang, Chem. Commun. (2007) 1215.
[4] M.A.Q. Khan, S.A. Ahmed, B. Catalin, A. Khodadoust, O. Ajayi, M. Vaughn, Environ. Toxicol. 21 (2006) 513.
[5] A. Smara, R. Delimi, E. Chainet, J. Sandeaux, Sep. Purif. Technol. 57 (2007) 103.
[6] D. Mohan, K.P. Singh, Water Res. 36 (2002) 2304.
[7] Y. Xing, X. Chen, D. Wang, Environ. Sci. Technol. 41 (2007) 1439.
[8] S.B. Lalvani, T. Wiltowski, A. Hubener, A. Weston, Carbon 36 (1998) 1219.
[9] Z. Reddad, C. Gerente, Y. Andres, P. Cloirec, Environ. Sci. Technol. 36 (2002) 2067.
[10] D.D. Das, R. Mahapatra, J. Pradhan, S.N. Das, R.S. Thakur, J. Colloid Interface Sci. 232 (2000) 235.
[11] J. Fang, Z. Gu, D. Gang, C. Liu, E.S. Ilton, B. Deng, Environ. Sci. Technol. 41 (2007) 4748.
[12] S.B. Lalvani, T. Wiltowski, A. Hubener, A. Weston, Carbon 36 (1998) 1219.
[13] J.C. Yu, L.Z. Zhang, Chem. Mater. 14 (2002) 4647.
[14] A. Ramesh, H. Hasegawa, T. Maki, K. Ueda, Sep. Purif. Technol. 56 (2007) 90.
[15] H.H. Murray, Appl. Clay Sci. 17 (2000) 207.
[16] J. Wang, D.M. Zhang, T.R. Lawson, R.A. Bartsch, Talanta 78 (2009) 477.
[17] J.M. Gong, T. Liu, X.Q. Wang, X.L. Hu, L.Z. Zhang, Environ. Sci. Technol. 45 (2011) 6181.
[18] J. Beltrán-Heredia, J. Sánchez-Martín, J. Hazard. Mater. 164 (2009) 713.
[19] L. Liu, C. Li, C.L. Bao, Q. Jia, P.F. Xiao, X.T. Liu, Q.P. Zhang, Talanta (2012), http://dx.doi.org/10.1016/j.talanta. 2012.02.051.
[20] Q.M. Ji, S. Acharya, P. Hill, A. Vinu, S.B. Yoon, J.S. Yu, K. Sakamoto, K. Ariga, Adv. Funct. Mater. 19 (2009) 1792.
[21] T.Y. Ma, X.J. Zhang, Z.Y. Yuan, J. Phys. Chem. C 113 (2009) 12854.
[22] J.B. Fei, Y. Cui, X.H. Yan, W. Qi, Y. Yang, K.W. Wang, Q. He, J.B. Li, Adv. Mater. 20 (2008) 452.
[23] L.S. Zhong, J.S. Hu, H.P. Liang, A.M. Gao, W.G. Song, Adv. Mater. 18 (2006) 2426.
[24] C.A. Oliveira, D.I. Petkowicz, A. Smaniotto, Water Research 38 (2004) 3699.
[25] J. Dong, Z.H. Xu, S.M. Kuznicki, Adv. Funct. Mater. 19 (2009) 1268.
[26] S.Y. Shin, J.S. Jang, Chem. Commun. (2007) 4230.
[27] V. Chandra, J. Park, Y. Chun, J.W. Lee, I. Hwang, K.S. Kim, ACS Nano 4 (2010) 3979.
[28] X.Y. Li, Z.J. Si, Y.Q. Lei, X.N. Li, J.H. Tang, H.J. Zhang, Cryst. Eng. Comm. 13 (2011) 642.
[29] J. Liu, S.Z. Qiao, Q.H. Hu, G.Q. Lu, Small 7 (2011) 425.
[30] T. Sen, I.J. Bruce, T. Mercer, Chem. Commun. 42 (2010) 6807.
[31] W.R. Zhao, H.R. Chen, Y.S. Li, L. Li, M.D. Lang, J.L. Shi, Adv. Funct. Mater. 18 (2008) 2780.
[32] Y.F. Zhu, E. Kockrick, T. Ikoma, N. Hanagata, S. Kaskel, Chem. Mater. 21 (2009) 2547.

[33] T.Y. Guo, Y.Q. Xia, J. Wang, M.D. Song, B.H. Zhang, Biomaterials 26 (2005) 5737.
[34] A.H. Chen, C.Y. Yang, C.Y. Chen, C.W. Chen, J. Hazard. Mater. 163 (2009) 1068.
[35] Q. Li, H.J. Su, T.W. Tan, Biochem. Eng. J. 38 (2008) 212.
[36] P. Gunawan, R. Xu, Chem. Mater. 21 (2009) 781.
[37] K.Q. Li, Z. Zheng, Y. Li, J. Hazard. Mater. 181 (2010) 440.
[38] N.N. Nassar, J. Hazard. Mater. 184 (2010) 538.
[39] A. Aklil, M. Mouflih, S. Sebti, J. Hazard. Mater. 112 (2004) 183.
[40] H.Z. Freundlich, Phys. Chem. 57 (1906) 387.
[41] I. Langmuir, J. Am. Chem. Soc. 40 (1918) 1361.
[42] I.I. Salame, T.J. Bandosz, J. Colloid Interface Sci. 264 (2003) 307.
[43] A. Ramesh, H. Hasegawa, T. Maki, K. Ueda, Sep. Purif. Technol. 56 (2007) 90.
[44] Y.S. Ho, G. McKay, Chem. Eng. J. 70 (1998) 115.
[45] A.K. Bhattacharyal, T.K. Naiya, S.N. Mondal, S.K. Das, Chem. Eng. J. 137 (2008) 529.
[46] D. Zhang, Z. Liu, S. Han, C. Li, B. Lei, M.P. Stewart, J.M. Tour, C. Zhou, Nano Lett. 4 (2004) 2151.
[47] X.F. Liang, W.G. Hou, Y.M. Xu, G.H. Sun, L. Wang, Y. Sun, X. Qin, Colloids and Surfaces A: Physicochem. Eng. Aspects 366 (2010) 50.
[48] J.R. Rangel-Mendez, R. Monroy-Zepeda, E. Leyva-Ramos, P.E. Diaz-Flores, K. Shirai, J. Hazard. Mater. 162 (2009) 503.